Antarctic Research, Vol. 2, No. 2, 1~14, December 1991

STRATIGRAPHY, DENSITY AND CRYSTAL STRUCTURE OF FIRN-ICE AT DE08—A VERY HIGH ACCUMULATION SITE ON LAW DOME, ANTARCTICA

Li Jun[1], N.W. Young and C.W. Wookey[2]

[1]*Lanzhou Institute of Glaciology and Geocryology, Academia Sinica, Lanhzou 730000, Cnina*

[2]*Antarctic Division, Channel Highway, Kingston TAS 7050, Australia*

Abstract An approximately 195 mm diameter firn / ice core, 234 m long, was thermally drilled in 1987 austral summer at DE08 (66°43′S, 113°12′E) on Law Dome, East Antarctica, where the accumulation rate is about 1200kg/(m²·a); 10m ice temperature is about −18.8 °C. Analysis was mainly made at the site immediately after drilling. The snow stratigraphy at DE08 is characterised by the lack of coarse-grained snow and other distinct visible feature normally corresponding to annual layers. There is a smooth transformation from fine-grained snow at shallow depth to ice at about 80–90m which is greater than that at most other polar locations due to its abnormally high accumulation rate. According to the marked change in the trend of density with depth and in the crystal properties four stages of the transformation of snow to ice and development of crystal structure can be distinguished; settling stage (0–10m); sintering stage (10–90m); rapid crystal growth stage (90–170m); and dynamic metamorphism stage (170—234m). The rates of densification and crystal growth from the surface to the depth of the firn-ice transition closely depend on the general temperature. Below the transition zone, the crystal growth rate is higher by a factor of 4.3 in comparison with that at other sites. The very high vertical strain rate at DE08 compared to that at the other sites suggests that the crystal growth rate in the ice layer may increase by the associated deformation.

Key words firn/ice core, stratigraphy, Law Dome.

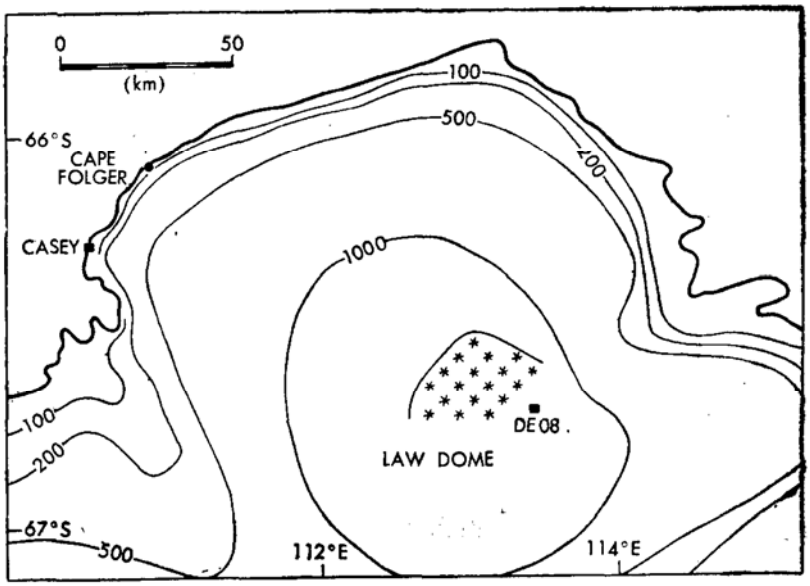

Fig. 1. Map of Law Dome Ice Cap showing location of DE08 drill site. Starred area is a dry snow zone delimited by Xie (1986).

Introduction

DE08 is located 16 km east of the summit of Law Dome, Antarctica, at latitude 66°43′19″S, longitude 113°11′58″E, with a surface elevation of 1250 m a.s.l. and total ice thickness about 1179 m (Fig. 1). In January 1987, a 234 m long, 195 mm diameter core was thermally drilled at DE 08. The following measurements and observations were made on-site as the drilling progressed: stratigraphy, solid D. C. electrical conductivity, density, crystal size and c-axis orientation. Thin-sections were cut, prepared and photographed immediately after drilling to avoid crystal modification by core relaxation and prolonged storage and transport. The in-situ ice temperature-depth profile was measured in the borehole following the drilling.

The primary chronology of the core is derived from the solid electrical conductivity measurements (Wookey, in preparation) which gives a mean accumulation rate for the last 50 years of 1200 kg / (m^2•a). This is close to the value of 1300 kg / (m^2•a) from cane measurements during the period from May 1984 to December 1987. The 10 m ice temperature is approximately -18.8°C (Etheridge and Wookey, 1988).

Sampling and measurement procedure

When a core section was retrieved from the thermal drill, a 10 mm thick layer was removed from a side of the section using an electric planer to give a clean flat surface. A stratigraphic description was made from the observations of visible features on a light box. ice lenses, that are artifacts prepared after infiltration of melt water during the thermal drilling, were put to about 40 m depth and ignored in this analysis. Density is calculated from measurements of length, diameter and mass of core samples turned to a cylindrical shape on a lathe. For the upper part of the core, samples were selected from the sections that were not visibly affected by melt water infiltration. Thin sections were prepared and photographed for investigations of bubble and crystal properties. Dodecane was used as a filler to support the firn/ice matrix during cutting on a vacuum stage microtome using the technique used by Alley (1980). Crystal c-axis orientation was measured on a Rigsby stage (Langway, 1958).

Crystal size is calculated as an average value for 100 crystals selected at random in a thin-section. A sample area in the thin-section of 1200–2400mm^2 is generally used. A set of rectangular coordinates is superimposed on a photograph of the thin-section. Pairs of numbers from a random number generator are used to define a coordinate point in the section. Measurements are then made on a crystal containing that point. The area of each crystal is calculated assuming it has an elliptical shape with major and minor axes given by the diameter of the smallest circumscribed circle D_c and the diameter of the largest inscribed circle D_i respectively. The sphericity of a crystal is defined as a ratio D_i / D_c. The sampling technique described here gives a weighted mean area because the probability of selecting any individual crystal is proportional to the area of the crystal.

In order to compare crystal size measurements presented here with earlier measurements by Gow (1975), additional measurements were made on a set of seventeen thin-sections from the LJ24 core using his technique (Gow, 1969). Average crystal size for these sections varies from 0.2 to 3.6mm^2. The relationship of crystal size measured by Gow's technique, S_g, to that measured by the technique presented here, S_l, can be approximated by

$$S_g = 1.148\ (S_i)\ 0.733 \quad (1)$$

with a correlation coefficient of 0.984 for the seventeen sections. Further work is required to determine if this relation is independent of any effect of ambient conditions at the site and sample age or depth. The mean diameter of air bubbles is defined as the geometric mean of the average long axis for 100 bubbles and the average short axis of the same 100 bubbles. The specific area of the internal free surface (ice-air contact area) and of the solid ice crystal boundary (ice-ice contact area) are determined from the following relation (Smith and Guttman, 1953)

$$S = 2N / L \quad (2)$$

where L is the total length of the lines drawn on the photograph and N is the number of intersections of the crystal boundaries (surfaces) with the lines. In this study a series of parallel lines was drawn on the photograph to give a total length of 200 mm. Specific area varies inversely as the crystal diameter (Narita and others, 1978).

Results and Discussion

1. *Stratigrayhical observations of snow pits*

The stratigraphy observed in two snow pits, 2.1 and 3.8 m deep, at DEO8 at different times is shown in Figure 2. The snow stratigraphy consists only of fine-grained snow except for one thin layer (a few millimetres thick) of fine deep-hoar. The lack of coarse material produces a very simple stratigraphy. The absence of any thick ice layers (greater than 2 mm thick) over the 1-2-year accumulation represented in the pit suggests that the site is in the dry-snow zone (Benson, 1962; Paterson, 1981; Xie, 1986).

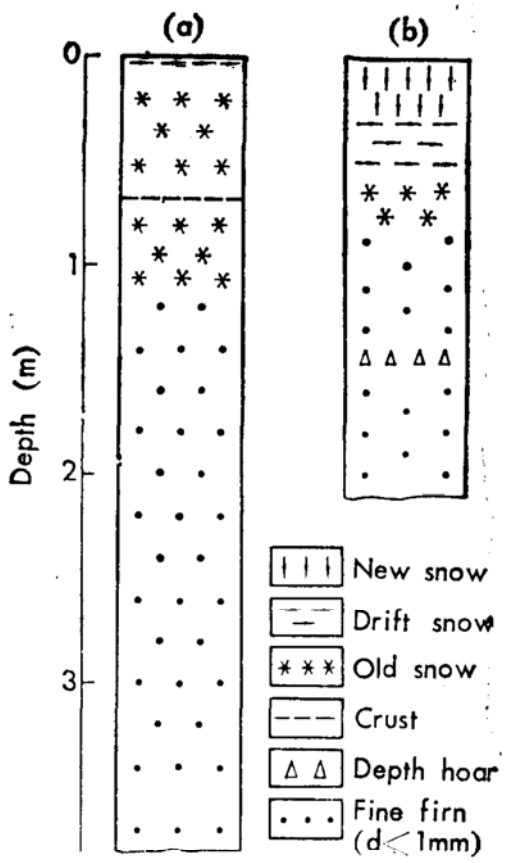

Fig. 2. Snow stratigraphic of DE08 pits dug on 16 / 1 / 1987 (a) and 5 / 4 / 1987 (b).

2. *Visible features of the core*

A gradual increase in crystal size could be observed along the core with depth and the firn transformed to ice below about 80 m. There is no apparent alternation of fine and coarse firn. The zone where the interconnected air passages in the firn are close-off to form individual bubbles could be observed. Below 80–90 m the bubbles gradually assume a spherical shape and become smaller with depth. Crusts could be easily distinguished along the length of the core. Most of them are transparent, less than 1 mm thick, formed under the influence of solar radiation during the summer months. By contrast, Alley and Koci (1988) found in snow pit at Site A in Greenland than most crusts become indistinct by about 2 m depth as a result of diagenetic changes. At DE08, the frequency of crusts decreases below about 100 m depth with pronouncedly increasing growth rate compared to that at shallower depth.

Figure 3 gives a schematic representation of the stratigraphy below 10 m together with the mean bubble diameter and number of crusts per depth interval. The number of crusts is calculated per metre increment in ice equivalent and then smoothed by taking a running mean over a 10 m

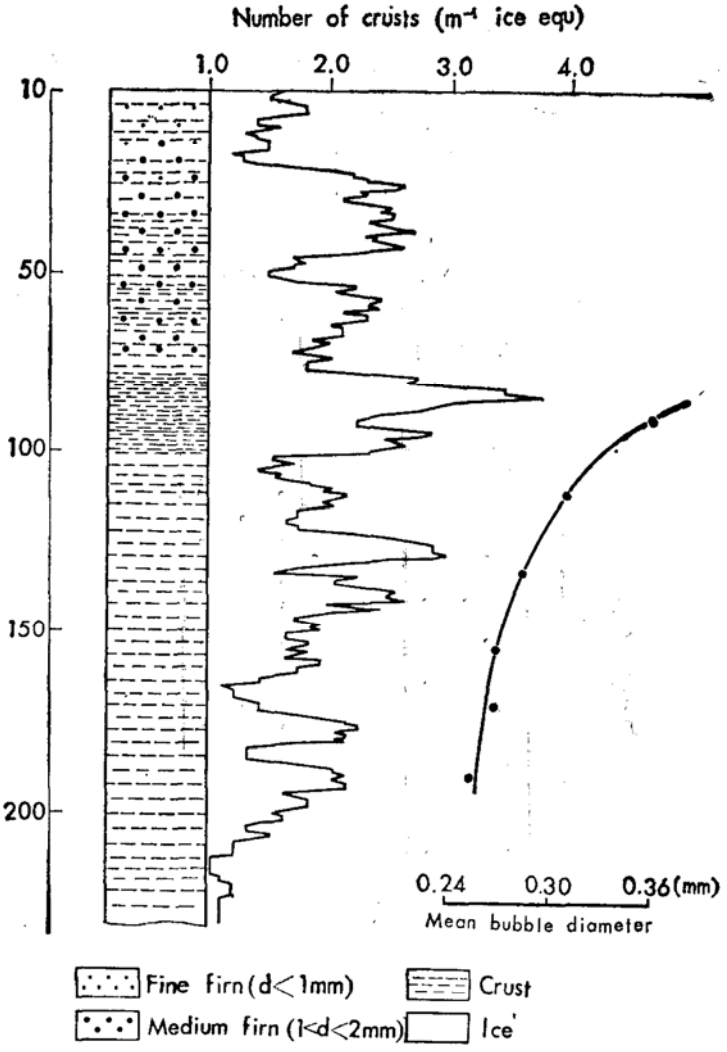

Fig. 3. Schematic stratigraphy of the DE08 core below 10 m depth, the number of crusts in a depth increment (1m ice equivalent increments, smoothed with a 10m running mean), together with mean bubble diameter versus depth.

Table 1. Firn—ice transition depth.

Site	Transition depth (m)	Accumulation rate ($kgm^{-2}a^{-1}$)	Mean annual temperature (°C)	Reference
Wilkes S2	38	130	−19	Paterson 1981
Roi Baudouin	46	380	−15	Paterson 1981
Little America	51	220	−24	Paterson 1981
Agassiz ice field	53	165	−25	Paterson 1981
Inge Lehmann	60	100	−30	Paterson 1981
Devon ice cap	62	220	−23	Paterson 1981
Byrd	64	140	−28	Paterson 1981
Site 2	66	410	−25	Paterson 1981
Maudheim	67	370	−17	Paterson 1981
Dye 3	65−70	490	−19	Paterson 1981
Camp Century	68	320	−24	Paterson 1981
Crete	68	250	−30	Paterson 1981
Milcent	66−70	480	−22	Paterson 1981
Law Dome summit	70	643	−21.3	Etheridge&others 1988
Siple	72−76	500	−24	Stauffer & others 1985
Site A	75−80	261	−29.5	Alley 1988
DE08	80−85	1200	−18.8	this work
Vostok	100	22	−57	Paterson 1981
Dome C	100	36	−54	Alley 1980

interval (in ice equivalent). Photographs of air bubbles at four different depths are given in Figure 4 (see p. 83)

3. Density-depth profile

The density-depth profile measured on samples from the core is shown in Figure 5. Density values from the snow pits, calculated as the mean values over 0.5 m intervals, are included to provide near-surface values. Three distinct depth zones can be delineated by significant breaks in the trend of density with depth at approximately 10 m and 90 m where the corresponding density is 580 and 860 kg / m^3 respectively. In the middle zone the trend can be closely approximated by a linear relation, but in the upper and lower zones the relation is non-linear. Benson (1959) and Gow (1968) found similar divisions and approximations for sites in Greenland and for Byrd, Antarctica.

The density-depth profile is approximated by the following functions:

$$\rho = \rho_i - 0.543 \exp(-0.049\, z) \qquad z < 10 \text{ m} \qquad r = 0.949 \qquad (3)$$

$$\rho = \rho_i + 0.0035\, z \qquad 10 < z < 90 \text{ m} \qquad r = 0.989 \qquad (4)$$

$$\rho = \rho_i - (4517\, z) - 2.516 \qquad 90 < z < 232 \text{ m} \qquad r = 0.964 \qquad (5)$$

where ρ is density (kg/m^3), z—depth (m), ρ_i—density of pure ice (918 kg/m^3) and r is a correlation coefficient. The three zones defined above are consistent with the three zones referred to by workers in describing the densification of cold dry snow (e.g. Bader 1965; Benson, 1962, Gow; 1975; Paterson, 1981). The boundaries of the three zones are typically set at densities of 550 and 830

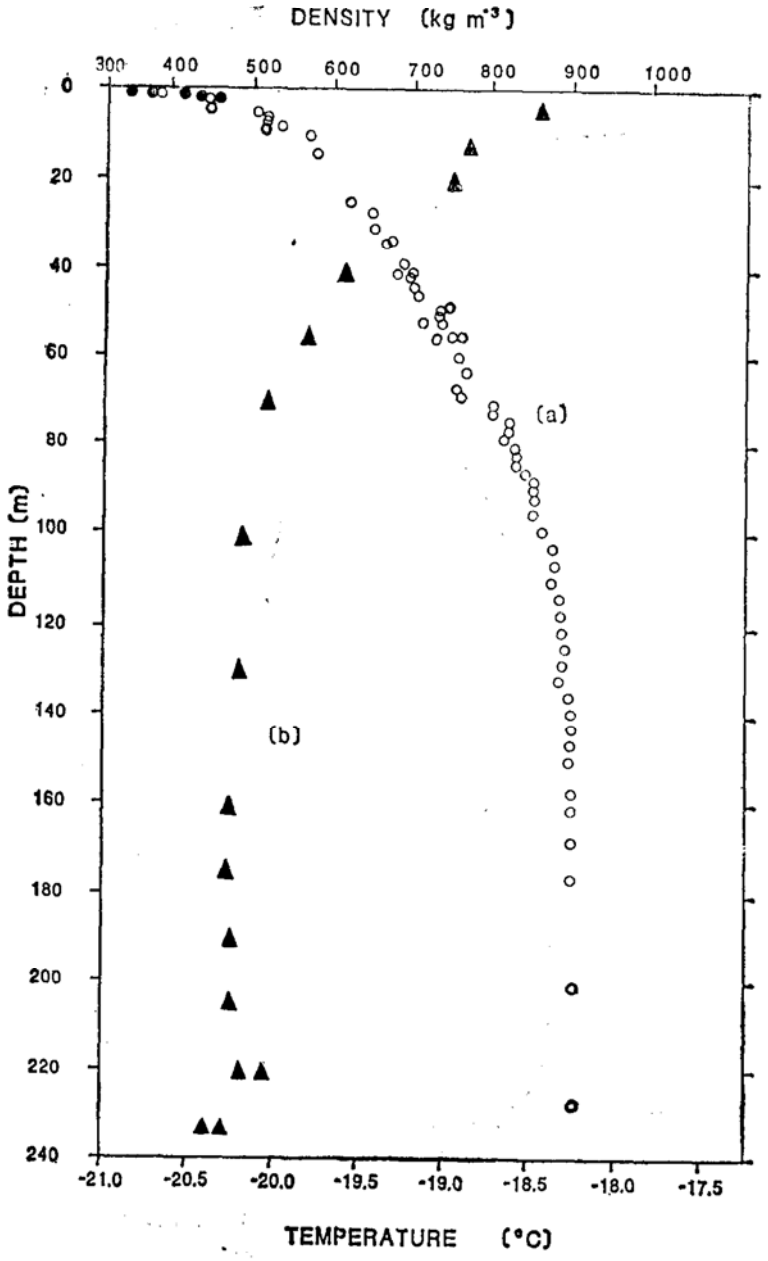

Fig. 5. Density-depth profile (a) and temperature-depth profile (b) for DEO8. Solid circles represent the density measurements taken at snow pits. Temperature data are cited from Etheridge and Wookey 1988.

kg/m³, and the dominant mechanisms of densification are described as grain settling in the upper zone, sintering in the middle zone and bubble compression in the ice.

The density-depth profile reflects the prevailing surface temperature and accumulation rate. In general the smaller the accumulation rate or higher the temperature, the smaller the increment of depth for a given increment of density. A useful parameter is the depth to the firn-ice transition. Table 1 presents measured values for a selection of sites. Except for the very cold locations of Vostok, Dome C and South Pole, DE08 has the largest Firn-ice transition depth. Gow (1975) summaried the data from ten stations where the 10m snow temperature ranges from —15°C (Roi Bau-

douin) to —57°C (Plateau). He found the temperature dependence of densification could be clearly demonstrated in the time needed to transform snow into ice at the different temperatures. There is a good linear relation between time required to reach the snow-ice transition and the 10m temperature of the snow. At DE08, the 10 m snow temperature is —18.8°C ; the age at the depth of firn-ice (80—90m) is around 50 years. This is closely fitted to the result of Gow (1975) as indicated in Figure 6.

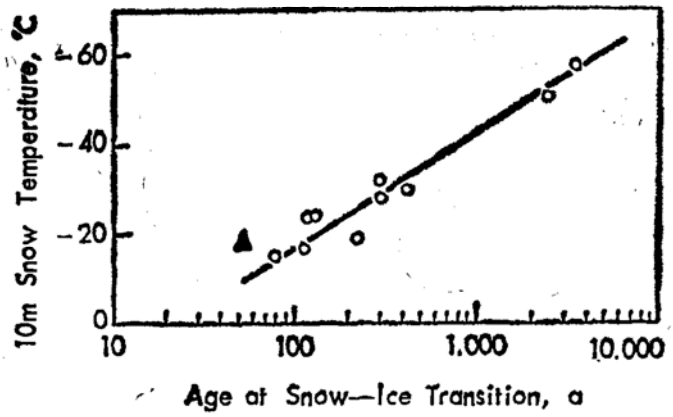

Fig. 6. Relation between age of snow-ice transition and snow temperature at 10m depth. Open circles indicate data from Gow (1975). Solid triangle indicates data for DEO8.

4. Crystal structure

Photographs of thin-sections showing the crystal structure from 8 different depths are given in Figure 7 (see p. 84~85) The crystals in recently deposited snow (Fig. 7a, 1 m depth) are generally separated, with an irregular shape and sharp points. With increasing depth the crystals tend to be roughly spherical with increasing inter-crystal contact area (Fig. 7b, 10 m). Bonding or necking occurs between crystals because of sintering (Fig. 7 c, 30 m). Then the bonds thicken, the spaces around them fill in and the firn begins to transform to ice with polygonal crystals (Fig. 7 d, 82m). Below that, in association with a more rapid growth of the crystals, the simple polygonal shape with linear boundaries is gradually replaced by the more complex shape of the dynamo-metamorphic structure, which exists below about 170m depth (Fig. 7e, 124 m; Fig. 7 f, 157 m; Fig. 7g, 184 m; Fig. 7h, 233m). Variations in crystal size, sphericity and specific area are another indications for the changes described above.

The crystal size-depth profile is shown in Figure 8 a. The mean crystal area increases linearly with depth in two stages. Below about 94m there is a sharp change in the gradient of crystal size with depth, indicating an increase in growth rate. Below 170 m the crystal size fluctuates about the general trend.

The sphericity-depth profile is shown in Figure 8c. For crystals with a circular cross-section the sphericity is 1 and for regular hexagons is 0.87 . All the measured sphericities are less than 0.75 and mostly less than 0.65, indicating that many crystals have cross-sections far from circular. There is a rapid increase near the surface to a maximum of 0.75 at 10 m depth, then a sharp decrease to about 0.65 at 25-30 m and a more gradual decrease to value near 0.55 at the bottom of the core. The increase in sphericity in the upper 10 m is consistent with the observed rounding of grains in the upper layers. The decrease below 10 m would appear to be related to the shape change

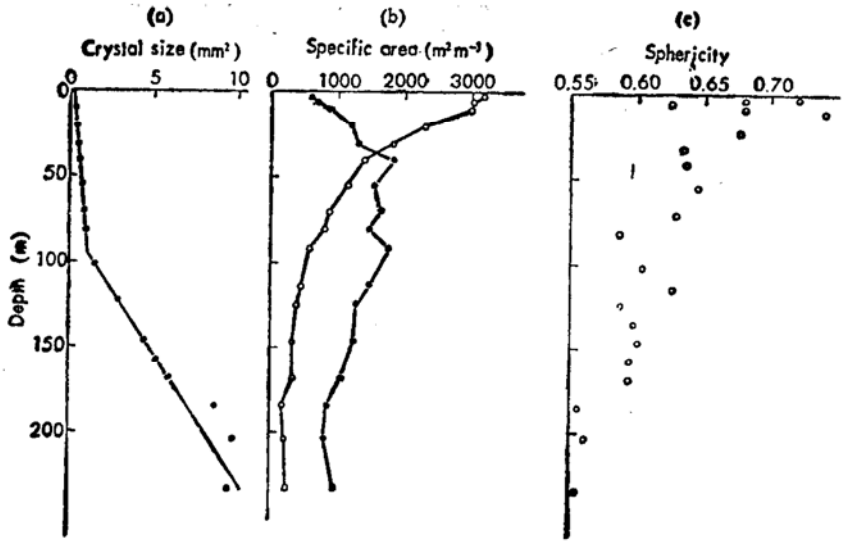

Fig. 8. Crystal properties for DE08: a. Crystal size versus depth. The two lines are drawn by inspection; b. Specific area versus depth. Solid circles show ice-ice crystal contact area, and open circles show free surface area; c. Sphericity-depth profile.

associated with the development of bonds or necking between crystals. As the crystals assume a polygonal shape, they tend to be slightly elongate. If any part of a crystal boundary becomes concave, then the sphericity would decrease further. such as occurs in the dynamo-metamorphosed ice. Figure 8 b shows the specific area measurements for the ice-ice crystal boundary and the internal free surface. The largest value of the free surface and the smallest value of the crystal boundary are found near the top of the core which is consistent with the crystals being well separated by small inter-crystal contact. The internal free surface decreases to the bottom of the core, whereas the ice-ice specific area initially increases to a maximum value between 50-90m depth and thereafter decreases. Both specific areas tend to be constant towards the bottom of the core. The increasing ice-ice specific area in the upper 50-60 m reflects two effects: the increasing density of the firn and the increasing proportion of ice-ice contact on the crystal boundary.

5. C-axis orientation

C-axis orientation fabric diagrams for eight different depths are shown in Figure 9. The pattern appears to be nearly random from the surface to about 170 m depth. From there to the bottom of the core there is some tendency to a central clustering with few subhorizontal axes. This tendency corresponds to the development of a complex crystal structure (Fig. 7 g and h), suggesting that deformation is beginning to have an effect on the structure.

The change in crystal properties around 170 m depth suggests another subdivision of the core additional to the divisions defined by the density-depth profile. The depth interval 90–233 m is sub-divided into two zones: 90–170 m where rapid crystal growth occurs in the ice, and 170–233 m where dynamic metamorphism begins to take effect.

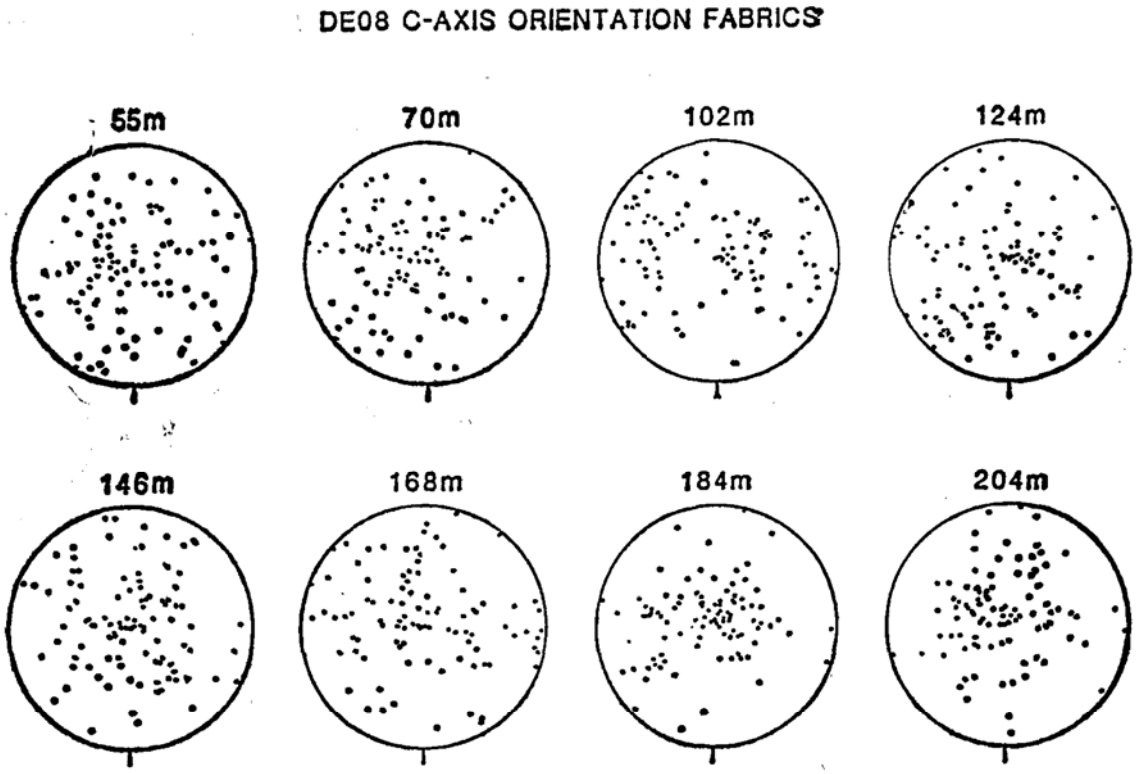

Fig. 9. C-axis orientation fabric diagrams for DE08. Data for 55 m depths were measured from vertical thinsection then rotated 90°. The other fabrics were measured on horizontal thin-sections.

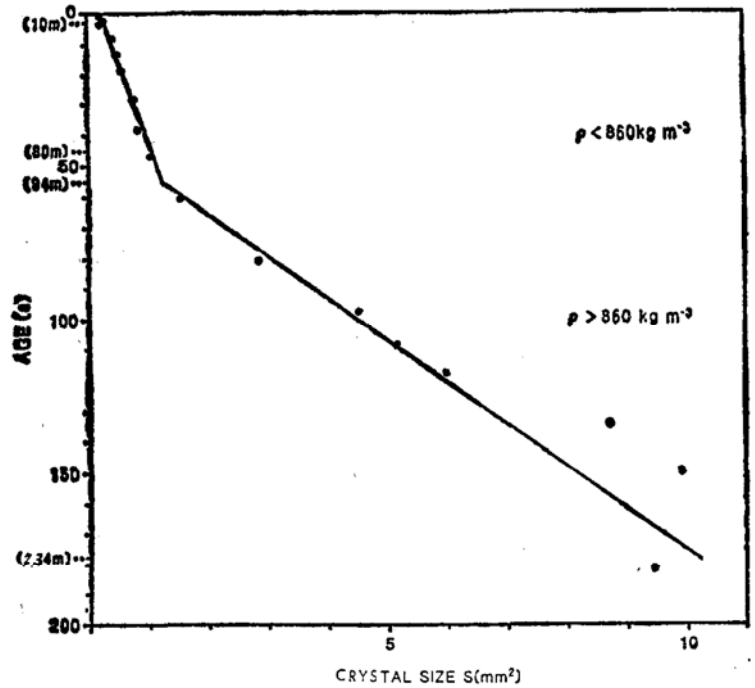

Fig. 10. Crystal size versus age for DE08. The two lines were fitted by least squares.

Crystal size is plotted against the snow age in Figure 10. The crystal size increases essentially linearly with the age for the first 50 years, which corresponds to the depth interval 0–90 m. But below 94 m depth (age–55 years), the growth rate increases significantly, by a factor of about 4.3.

The trend of crystal size with age is approximated by two regression lines in Figure 10, one corresponding to the growth rate in firn and the other to the growth rate in ice. In the firn, the growth rate is constant from the surface downwards. There is no evidence of increasing growth rate in the upper few metres, as found at other sites by Gow (1975) and Qin and others (1988). They suggest that an increasing growth rate in the near-surface layer would result from vapour diffusion along with strong temperature gradients and the exposure of the firn to this effect over a long period. At DE08, the accumulation rate is so high that the staying period of the firn near the surface is much shorter than that at low accumulation area, as indicated in Table 2, and that the firn is never exposed to such temperature effects for any significant period, and hence the crystals grow in close to an isothermal environment.

Table 2. Age of the snow at 3m depth.

Site	Age(a)	Reference
Plateau	40	Gow 1971
Dome C	32	Alley 1980
South Pole	17	Alley 1980
Inge Lehmann	11	Gow 1971
Litter America	9	Gow 1968
Byrd	7	Gow 1968
Camp Century	3	Gow 1971
DZ08	0.8	This work

The crystal size can be expressed as a function of time and temperature by

$$S^2 = S_0^2 + K_t \tag{6}$$

where S_0 is the initial crystal size (i.e. mean crystal cross-section area), S is the size after time t, and K is the growth rate which can be expressed by the Aarhenius relation

$$K = K_0 \exp(-E/RT) \tag{7}$$

where K_0 is a constant, R is the gas constant, T is the absolute temperature and E is the apparent activation energy for crystal growth (Gow, 1975). The value of E varies in a range from 42.3 to 48.6 kJ mol^{-1}, depending on the selection of data used by different authors (Gow, 1975, Paterson, 1981, Duval, 1985). The relation and data given by Gow (1975) is shown in Figure 11.

From the regression line shown in Figure 11 the growth rate in firn is 0.0179 mm^2 / a and the growth rate in ice is 0.0767 mm^2 / a. But to compare these values with Gow's data, allowance needs to be made for the bias in crystal size resulted from the difference in the techniques. Applying the relation to equation 1 gives the value 0.0181 mm^2/a in the firn. The regression line of growth rate against the inverse of temperature given by Gow (1975)predicts a value of 0.0224mm^2/a for a temperature of −18.8°C. The measured value is close to this predicted value, indicating the growth rate in the firn at DE08 is consistent with the relation described by equations 6 and 7. But the value in ice is much higher. Figure 5 shows the temperature-depth profile for DE08. The temperature decreases from approximately −18.5°C near the surface to −20.2°C around 100m and is almost isothermal to 230 m, where the minimum temperature of −20.3°C occurs. For this temperature range the predicted growth rate ranges from 0.0230 mm^2 / a for −18.5°C to 0.0199 mm^2 / a for −20.3°C. The effect of temperature cannot explain the large difference in the growth

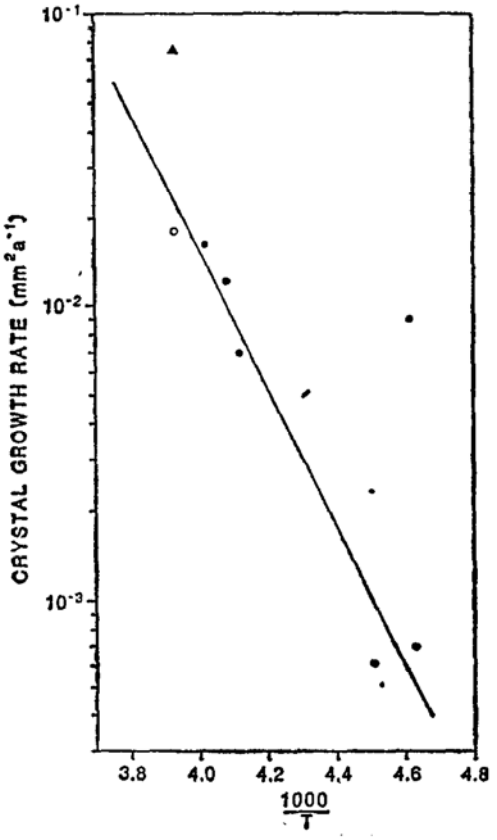

Fig. 11. Relation between crystal growth rate and temperature. Solid circles show data from Gow (1975). The values for the firn and ice from DE08 are shown as open circle for the firn and solid triangle for ice.

rates in firn and ice.

Alley (1986a and b) and Duval (1985) used measurements on deep ice cores from Greenland and Antarctica to extend the study of crystal growth rates from firn to ice. They restricted their work to the zone above the depth ,where shear deformation occurs and development of a c-axis fabric become significant. They concluded that the crystal growth rate obeys the same temperature relation in ice as in firn and that there is no change in growth rate across the firn / ice transition.

The sites investigated by Alley (1986a and b) and Duval (1985) have low accumulation rate, cold temperature and large ice thickness. By contrast, DE08 has a very high accumulation rate, smaller ice thickness and warmer temperature. Thus the vertical strain rate at DE08 would be much higher than that at the other sites. There is no large change in ice thickness immediately upstream of DE08 and the flow is close to planar. By assuming that the ice sheet is in steady state and that the strain rate is uniform with depth, an estimate of the vertical strain rate can be obtained from

$$\dot{\varepsilon}_z = -\frac{a}{\rho_i Z} \tag{9}$$

Table 3. Estimated vertical strain rate.

Site	$\dot{\varepsilon}_z$ (a^{-1})	Reference
Vostok	7×10^{-6}	Duval and Liboutry 1985
Dome C	1×10^{-5}	Duval and Liboutry 1985
South Pole	3.19×10^{-5}	Duval and Liboutry 1985
Mizuho.	3.68×10^{-5}	Duval and Liboutry 1985
Byrd	7.85×10^{-5}	Duval and Liboutry 1985
Camp Century	2.76×10^{-4}	Duval and Liboutry 1985
DE08	1.1×10^{-3}	This work

where a (kg / m^2•a) is the accumulation rate, Z is the equivalent ice thickness (m), and ρ_i is the density of ice (918 kg/m^3). Calculated values are given in Table 3, where it can be seen that the vertical strain rate at DE08 is one to two orders of magnitude greater than that at the other sites. This suggests that the strain rate and / or accumulated strain or stress may play a role in controlling the crystal growth rate. At DE08, the estimated accumulated vertical strain is around 5% at 90m depth and about 18% at the bottom of the core. The octahedral value of the strain at the corresponding depths is 3—4% and 13—15% respectively. The octahedral values depend on the strain configuration. For a plane flow regime the larger octahedral value is relevant, but if there is divergence locally at DE08, the octahedral value would be smaller.

From laboratory uniaxial compression experiments on ice, Jacka and Maccagnan (1984) found that ice crystal diameter increases during the creep stage when strain rate increases from minimum to maximum teritary value. The crystal growth in diameter ceased once, the constant tertiary flow rate was attained. In further experiments Jacka (1984) used ice with a range of initial crystal sizes. He found that for the samples deformed under the same temperature and stress conditions, the crystal sizes attained approximately the same value at the termination of experiment in the tertiary creep stage, independent of whether the initial crystal size is larger of smaller than the final size. He concluded that tertiary ice flow may limit crystal growth to an equilibrium size. The experimental strain rate is three orders of magnitude greater than that at DE08, and total strain of the order of 30%. Additional work is needed to find the dependence of crystal size and growth rate on the effects of deformation in the ice sheet.

Conclusion

The snow stratigraphy at DE08 is characterized by the lack of coarse-grained material and any other distinct feature normally associated with annual layering or individual storm events. There is a smooth transformation from fine-grained snow at shallow depth to ice at about 80–90m. The firn-ice transition depth is greater at DE08 than at most other polar locations because of its abnormally high accumulation rate. Crusts can be distinguished through the total length of the core, but the frequency of occurence decreases below about 95m.

Marked changes in the trend of density with depth and in the crystal properties are used to define four stages in the transformation of snow to ice and development of crystal structure. The four stages and the corresponding depth zones are as follows: settling stage (0–10m); sintering stage (10–90m); rapid crystal growth stage (90–170m) and dynamic metamorphism stage (170–233m).

The rates of densification and crystal growth from the surface to the depth of the firn-ice transition closely depend on the general temperature (Gow, 1975), but the very high accumulation prevents the near-surface snow from being exposed to large temperature gradients or variations for any time period, so that the crystal grow in an almost isothermal condition. Below the firn-ice transition zone the crystal growth rate is higher by a factor of 4.3 in comparison with the results from other sites where there is no detectable change in growth rate with depth in the upper part of the ice sheet near the firn-ice transition. The very high vertical strain rate at DE08 compared to that at the other sites suggests that the crystal growth rate in the ice may increase by the associated deformation.

Acknowledgements We thank Dr. Jo Jacka, Glaciology Section of Antarctic Division, Department of Science and Technology, Australia, for his valuable discussion and Dr. Etheridge of the Glaciology Section for his help in the field and in Melbourne.

References

Alley, R. B. (1980): Densification and recrystallization of firn at Dome C, central East Antarctica, Ohio State University, *Institute of Polar Studies Report*, 77.

Alley, R. B. and Koci, B. R. (1988): Ice-core analysis at site A, Greenland: preliminary results, *Annals of Glaciology*, 10, 1—4.

Alley, R. B., Perepezko, J. H. and Bentley, C. R. (1986a): Grain growth in polar ice: I. Theory, *Journal of Glaciology*, 32 (112),415—424.

Alley, R. B., Perepezko, J. H. and Bentley, C. R. (1986): Grain growth in polar ice: II. Application, *Journal of Glaciology*, 32 (112): 425—433.

Bader, H. (1965): Theory of densification of dry, bubbly glacier ice, *CRREL Research Report*, 141.

Benson, C. S. (1959): Physical investigations on the snow and firn of Northwest Greenland 1952, 1953 and 1954, *SIPRE Research Report*, 45 pp.

Benson, C. S. (1962): Stratigraphic studies in the snow and firn of the Greenland ice sheet, *SIPRE Research Report* 70, 139 pp.

Duval, P. (1985): Grain growth and mechanical behaviour of polar ice, *Annals of Glaciology*, 6,79—82.

Etheridge, D. M. and Wookey, C. W. (1988): Ice core drilling at DE08, Law Dome, 1987, *Glaciology Section Internal Report*.

Etheridge, D. M., Pearman, G. I. and de Silva, F. (1988): Atmospheric trace-gas variations as revealed by air trapped in an ice core from Law Dome, Antarctica, *Annals of Glaciology*, 10,28—33.

Gow, A. J. (1968): Deep core studies of the accumulation and densification of snow at Byrd Station and Little America V, Antarctica, *CRREL Research Report*, 197, 45 pp.

Gow, A. J. (1969): On the rates of growth of grains and crystals in South Polar firn, *Journal of Glaciology*, 8 (53), 241—252.

Gow, A. J. (1971): Depth-time-temperature relationships of ice crystal growth in polar glaciers, *CRREL Research Report*, 300,18 pp.

Gow, A. J. (1975): Time-temperature dependence of sintering in perennial isothermal snowpacks, *IASH Publication* 114 (Symposium of Grindelwald 1974-Snow Mechanics), 25—41.

Jacka, T. H. (1984): Laboratory studies on relationships between ice crystal size and flow rate, *Cold Regions Science and Technology*, 10 (1),31—42.

Jacka, T. H. and Maccagnan, M. (1984): Ice crystallographic and strain rate changes with strain in compression and extension, *Cold Regions Science and Technology*, 8 (3), 269—286.

Narita, H., Norikazu, M. and Masayoshi, N. (1978): Structural characteristics of firn and ice cores drilled at Mizuho station, East Antarctica. *Memoirs of the National Institute of Polar Research, Special* Issue, 39, pp. 157—164.

Langway, C. C. Jr. (1958): Ice fabric and the universal stage, *SIPRE Technical Report*, 62.

Paterson, W. S. B. (1981): The physics of glaciers. Second edition, Oxford, Pergamon Press (Pergamon International Library).

Qin, D., Young, N. W. and Thwaites, R. J. (1988): Growth rate of crystals within the surface snow / firn layer in

Wilkes Land, Antarctica, *Annals of Glaciology*, 11.
Smith, C. S. and Guttman, L. (1953): Measurement of internal boundaries in three-dimensional structures by random sectioning, *Journal of Metals*, **5** (1), 81—87.
Stauffer, J., Schwander, J. and Oeschger, H. (1985): Enclosure of air during metamorphosis of dry firn to ice. *Annals of Glaciology*, 6,108—112.
Xie Zichu (1986): Ice formation and ice structure on Law Dome, Antarctica, *Annals of Glaciology* 6,150—153.

(received, 1990)

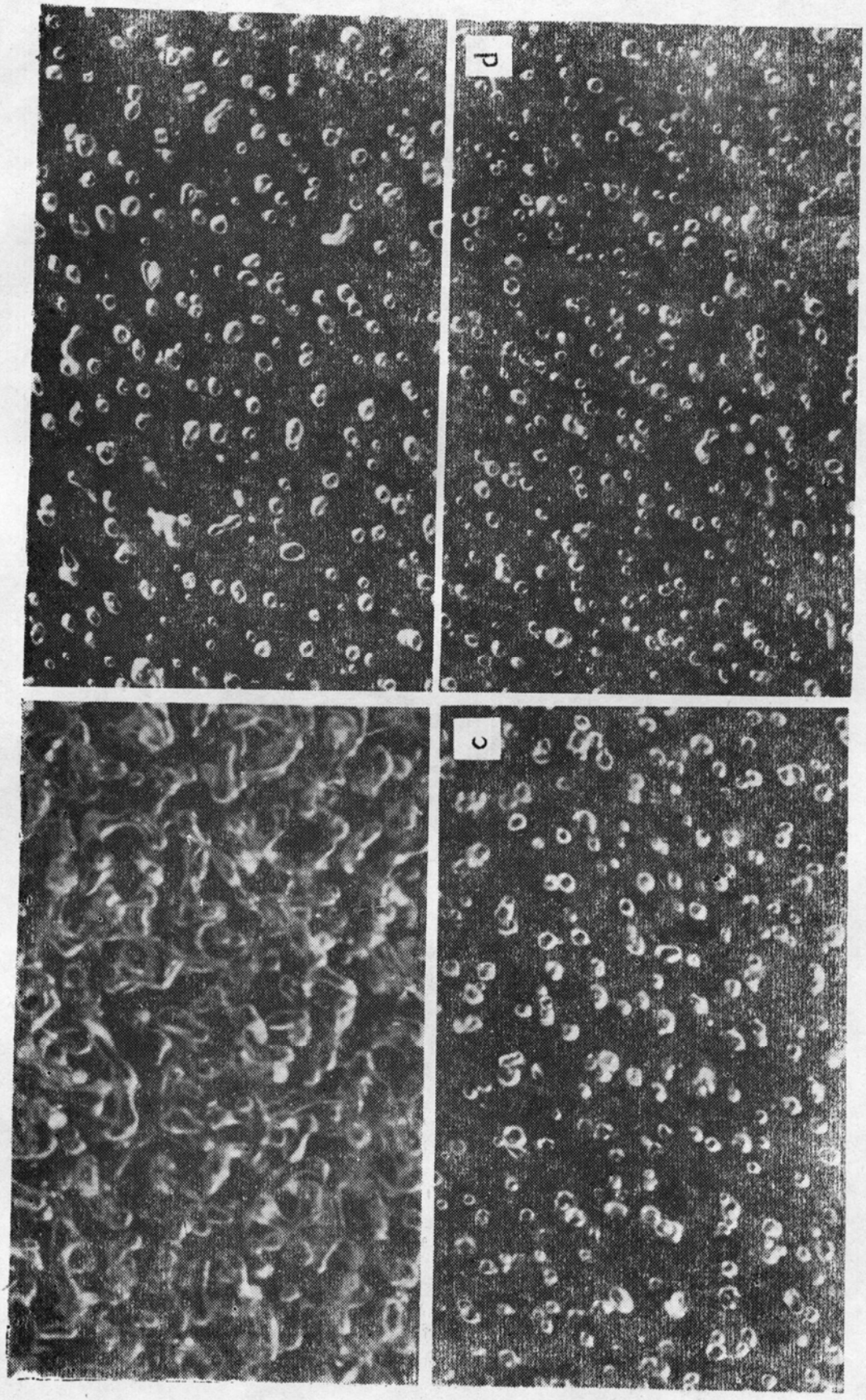

Fig. 4. Photographs of thin sections from DE08 for four different depths (a:81m, b:157m, c:184m, d:233m) showing bubble features.

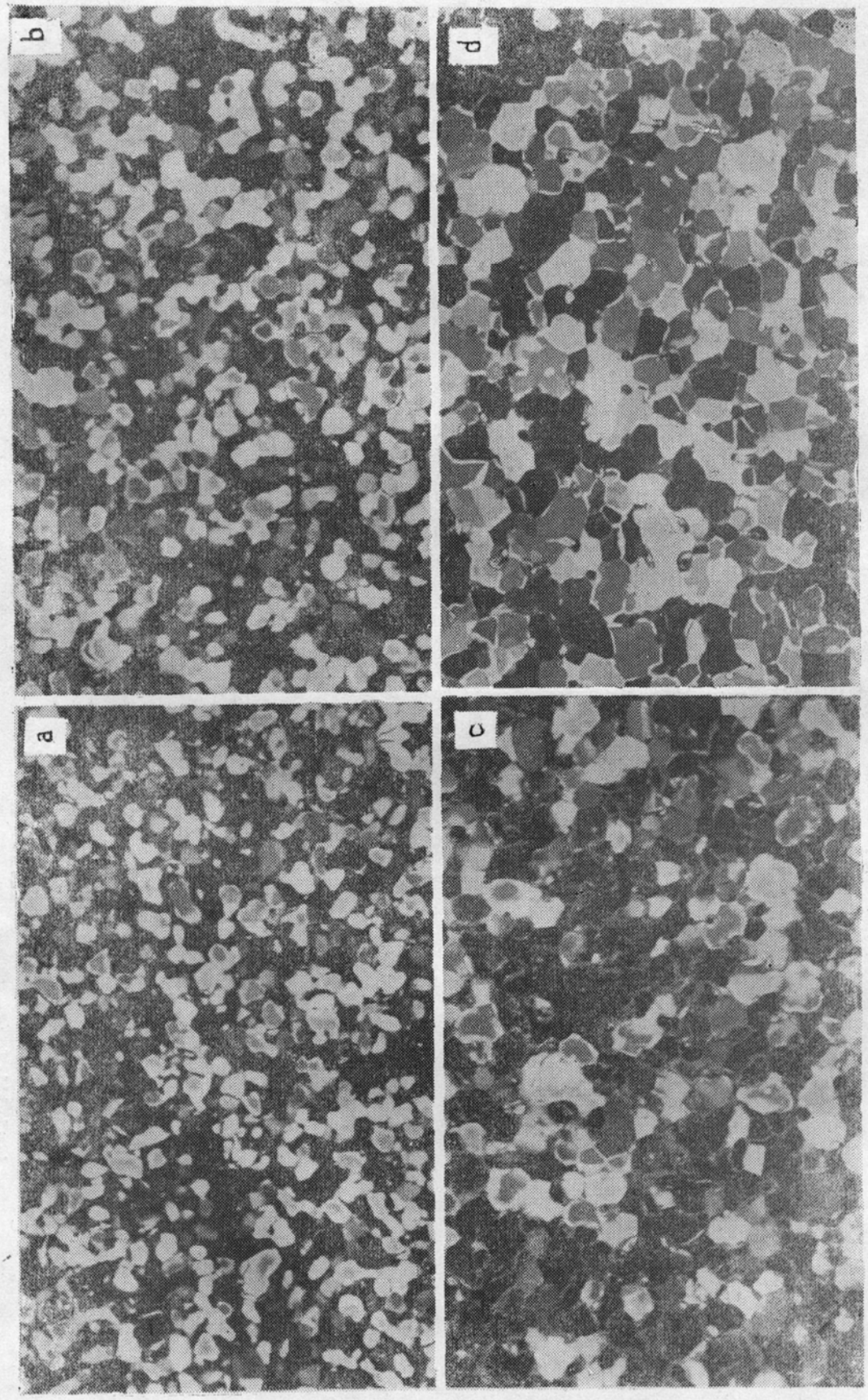
b
d
a
c

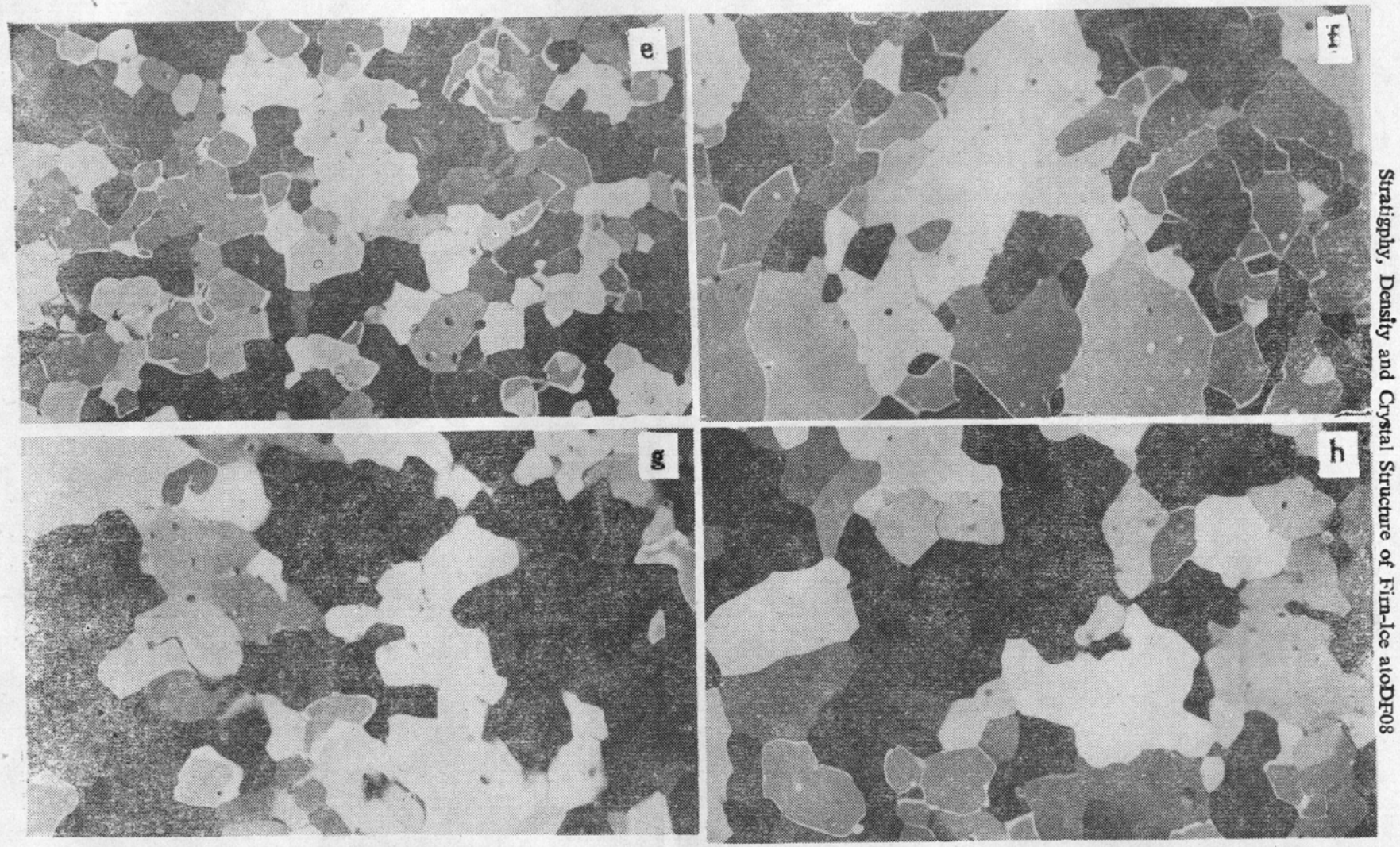

Fig. 7. Photographs of thin—sections from the DE08 core at eight different depths (a:1m, b:10m, c:30m, d:82m, e:124m, f:157m, g:184m, h:233m) showing the crystal structure. The photos for three top depths have a scale 1.5 times the magnification of the other photos.